Journal of Environmental Management 342 (2023) 118243

Contents lists available at ScienceDirect

Journal of Environmental Management

journal homepage: www.elsevier.com/locate/jenvman

Research article

Advanced thermal hydrolysis for biopolymer production from waste activated sludge: Kinetics and fingerprints

Luis Romero [a], Paula Oulego [a], Sergio Collado [a], Mario Díaz [a,*]

[a] Department of Chemical and Environmental Engineering, University of Oviedo, C/Julián Clavería s/n, E-33071, Oviedo, Spain

ARTICLE INFO

Keywords:
Advanced thermal hydrolysis
Biopolymers
Fingerprints
Hydrogen peroxide
Kinetics
Waste activated sludge

ABSTRACT

Waste activated sludge (WAS) is the main residue of wastewater treatment plants, which can be considered an environmental problem of prime concern due to its increasing generation. In this study, a non-energetic approach was evaluated in order to use WAS as a renewable resource of high value-added products. For this reason, WAS was treated by thermal hydrolysis, H_2O_2 oxidation and advanced thermal hydrolysis (ATH) promoted by H_2O_2. The influence of temperature, H_2O_2 concentration and dosing strategy on biomolecule production (proteins and carbohydrates), size distribution (fingerprints) and various physico-chemical parameters (VSS, total and soluble COD, soluble TOC, pH and colour) was studied. The results revealed a synergistic effect between TH and H_2O_2 oxidation, which led to a significant increase in the production of both proteins and carbohydrates. In this sense, the concentration of proteins and carbohydrates obtained during TH at 85 °C for120 min was found to be 1376 ± 9 mg/L (121 mg/gVSS$_o$) and 208 ± 4 mg/L (18 mg/gVSS$_o$), respectively. However, in the presence of 4.5 mM H_2O_2/gVSS$_o$ under the same process conditions, the concentrations of proteins and carbohydrates exhibited a significant increase of 1.9-fold and 3.1-fold, respectively. Besides, the addition of H_2O_2 promoted the transformation of hydrophobic compounds, such as proteins and or lipids, into hydrophilic compounds, which presented low and medium sizes. An increase in temperature improved the solubilization rate and the yield of biomolecules significantly. Besides, the analysis of the kinetics related to the dosing strategy of H_2O_2 suggested the existence of two fractions during WAS solubilization, one of them being easily oxidizable, whereas the other one was more refractory to oxidation. Thus, the value of k_{H2O2} for the first addition of 1 mM H_2O_2/g VSS$_o$ was 0.020 $L^{0.4}$ $mgH_2O_2^{-0.4}$ min^{-1}, while it was 4.3 and 8 times lower for the second and third additions, respectively.

Credit author statement

Luis Romero: Conceptualization, Data Curation, Investigation, Formal analysis Visualization, Writing-Original Draft.

Paula Oulego: Conceptualization, Methodology, Resources, Supervision, Validation, Writing - Review & Editing.

Sergio Collado: Methodology, Formal analysis, Validation, Resources.

Mario Díaz: Funding acquisition, Project administration, Supervision, Validation.

1. Introduction

Waste activated sludge (WAS) is a by-product generated in wastewater treatment plants (WWTP), which represents a major issue from a handling point of view due to the large volume generated in these facilities. Thus, around 13000 thousand tons (dry matter) were produced in the European Union in 2020 (Elshikh et al., 2022). In fact, the processing and disposal of WAS, accounts for 50% of the total water treatment cost (Appels et al., 2008). Hence, several methods were developed for WAS management, such as it use as agricultural fertilizers or landfill disposal (García et al., 2017). Nevertheless, the stringent environmental constrains, in terms of heavy metal and harmful substance content limit its application (Pathak et al., 2009).

Currently, anaerobic digestion is a widespread WAS treatment aimed at facilitating subsequent management steps (Kacprzak et al., 2017). This process involves the generation of biogas, which improves cost-effectiveness of the WWTP, by taking advantage of the energy generated through biogas combustion for both internal and external use. However, anaerobic digestion takes place over a long period of time and

* Corresponding author. Department of Chemical and Environmental Engineering, University of Oviedo, C/ Julián Clavería s/n, Oviedo, Asturias, ES E-33071, Spain.

E-mail address: mariodiaz@uniovi.es (M. Díaz).

https://doi.org/10.1016/j.jenvman.2023.118243
Received 28 March 2023; Received in revised form 18 May 2023; Accepted 22 May 2023
Available online 3 June 2023

pretreatment techniques (microwave, ultrasound, oxidative treatments, and alkaline or acid conditions) are needed to enhance the fermentation process (Geng et al., 2022; Qiao et al., 2020). Therefore, advanced strategies are necessary for the optimal valorisation of the WAS under the circular economy approach. Among them, thermal hydrolysis (TH) processes have proven to be very adequate since they disrupt WAS flocs, thus releasing intracellular and extracellular material (Jeong et al., 2019; Pilli et al., 2015). The conditions typically used in this process are severe, as temperature can be as high as 200 °C and pressure can reach 60 bar, leading to a significant increase in energy consumption (Abe et al., 2013). For this reason, different promoting or oxidizing substances can be used to perform this process at milder conditions. Among such substances are persulfate reagents, surfactants, enzymes and Fenton reagents (Erden and Filibeli, 2010; Gao et al., 2020; Lee et al., 2016; Shi et al., 2021).

Advanced thermal hydrolysis (ATH) is a novel WAS pretreatment which relies on the combination of steam injection with hydrogen peroxide (H_2O_2). In contrast to conventional TH, it benefits from the synergistic effect of these two factors, avoiding the use of catalysts and pH swings. In this way, milder are technically feasible, which minimizes energy consumption (Abelleira et al., 2012b). The mechanism whereby ATH occurs is detailed by Ngo et al. (2021). Firstly, it is explained the degradation of H_2O_2 into water and oxygen Eq. (1), and similarly into hydroxyl radicals Eq. (2). Subsequently, oxygen acts on the weak bonds between carbon and hydrogen in organic compounds, thus forming hydroperoxyl, alkyl and hydroxyl radicals Eqs. (3) and (4) (Bachir et al., 2001; Rivas et al., 1999).

$$H_2O_2 \rightarrow H_2O + \frac{1}{2}O_2 \quad (1)$$

$$H_2O_2 \rightarrow 2HO^{\cdot} \quad (2)$$

$$RH + O_2 \rightarrow R^{\cdot} + HOO^{\cdot} \quad (3)$$

$$RH + H_2O_2 \rightarrow R^{\cdot} + HO^{\cdot} + H_2O \quad (4)$$

Further reactions occur during the propagation stage of ATH (Eqs. 5–10), resulting in the formation of many other radicals, such as organic peroxyl radicals ($ROO^{\cdot}$). The reactions shown in Eqs. (1), (2) and (4) can also occur at the propagation stage if the reaction shown in Eq (10) takes place.

$$H^{\cdot} + O_2 \rightarrow HOO^{\cdot} \quad (5)$$

$$R^{\cdot} + O_2 \rightarrow ROO^{\cdot} \quad (6)$$

$$RH + ROO^{\cdot} \rightarrow R^{\cdot} + ROOH \quad (7)$$

$$ROO^{\cdot} \rightarrow R^{\cdot} + CO_2 \quad (8)$$

$$ROOH \rightarrow RO^{\cdot} + HO^{\cdot} \quad (9)$$

$$RH + HOO^{\cdot} \rightarrow R^{\cdot} + H_2O_2 \quad (10)$$

The presence of these oxidative compounds helps to break down the cell walls of WAS, which are resistant to TH at milder temperatures. Therefore, releasing the intracellular material and extracellular polymeric substances (EPS), mainly composed of proteins and carbohydrates (Lee et al., 2016; Urrea et al., 2016a), promotes the generation of methane during anaerobic digestion. However, as an alternative approach to biogas production, these compounds can be separated and utilized as a substrate for fermentations, or as components in the production of adhesives, fertilizers, or animal feed (Hwang et al., 2008; Tekin et al., 2014).

Within this framework, previous studies on ATH have highlighted its technological advantages including improving dewatering process, sludge pretreatment (disintegration degree) and post-treatment (organic matter removal). Additionally, ATH has demonstrated enhanced biogas production in terms of both quantities and qualities (Abelleira et al., 2012a, 2012b). Nevertheless, to the best of our knowledge, the impact of ATH on the production of biomolecules of interest (proteins and carbohydrates), as well as their characteristics (particle size distribution) and kinetics has not been previously analysed. This knowledge gap is noteworthy due to the significant presence of these compounds in the WAS and their high value added (Chen et al., 2007).

Therefore, the aim of this study was to evaluate the effectiveness of ATH as a pretreatment process for obtaining proteins and carbohydrates from WAS. The effect of various parameters, including H_2O_2 concentration, dosing strategy, and process temperature, was thoroughly analysed to identify the optimal operating conditions. Moreover, kinetic models were developed for the volatile suspended solids (VSS), the oxidant, and the biomolecules produced, and their size distribution (fingerprints) were also determined.

2. Material and methods

2.1. Sludge samples

The experiments were performed using WAS from the secondary treatment of a WWTP located in Asturias (Spain). Following its collection, the sludge was immediately stored at 4 °C to avoid degradation. The main characteristics of the WAS are shown in Table 1.

2.2. Analytical methods

Total suspended solids (TSS), VSS, sludge volume index (SVI), total and soluble chemical oxygen demand (TCOD and SCOD), and pH measurements were carry out according to Standard Methods (APHA, 2012). A TOC analyser (Shimadzu TOC-VCSH, Japan) was employed for total organic carbon (TOC) and inorganic carbon (IC) quantification.

Lowry method was employed to determine protein concentration, using bovine serum albumin (BSA) as standard (Lowry et al., 1951). Carbohydrate determination was performed by means of Dubois method, using glucose as standard (DuBois et al., 1956). H_2O_2 concentration was measured using metavanadate method (Nogueira et al., 2005), so a small aliquot of WAS was centrifuged and the supernatant immediately separated to be combined in equal parts with the metavanadate. All the analyses were performed in triplicate with standard deviation less than 6% with respect to the mean values.

Colour was measured as colour number (CN) in accordance with Eq. (11):

$$CN = \frac{SAC_{436}^2 + SAC_{525}^2 + SAC_{620}^2}{SAC_{436} + SAC_{525} + SAC_{620}} \quad (11)$$

Where SAC_i is the spectral absorption coefficient at a wavelength of 436, 525 and 620 nm.

A Thermoscientific Genesys 150 UV–visible spectrophotometer (Thermo Fisher Scientific, USA) was employed for the measurement of

Table 1
Main characteristics of the WAS used in the experiments.

Parameter	Units	Value
pH		7.03 ± 0.2
Colour		0.02 ± 0.01
TCOD	mg O_2/L	17278 ± 24
SCOD	mg O_2/L	237 ± 5
TSS	g/L	14.4 ± 0.2
SVI	ml/g	90 ± 1
VSS	g/L	11.4 ± 0.2
Proteins[a]	mg/L	40 ± 2
Carbohydrates[a]	mg/L	20 ± 6
TOC[a]	mg C/L	226 ± 21
IC[a]	mg C/L	56 ± 2

[a] Referred to soluble concentration.

proteins, carbohydrates, H_2O_2 concentration and CN. In the case of TCOD and SCOD, a DR2500 spectrophotometer (Hach Company, USA) was used for these measurements. For pH measurement, a Sension + PH3 (Hach Company, USA) pH meter was employed.

2.3. Experimental setup

TH and ATH experiments were carried out in a 1 L reactor using a magnetic stirrer Agimatic-N with heating, which was equipped with an EKT Hei-Con digital electronic contact thermocouple for temperature control. The volume of sludge used was 700 ml and the stirring speed was set at 150 rpm for all experiments.

TH tests were carried out at temperatures within the 55–85 °C range, which has been used in previous studies for the thermal activation of oxidants (Kim et al., 2016; Lee et al., 2016). For ATH experiments, the reactor was preheated to the desired temperature, H_2O_2 was added after a 60 min after heating period. Then, samples were withdrawn periodically throughout the experiment.

85 °C and 3 mM H_2O_2/g VSS_o were selected as reference conditions. Different parameters were modified, such as peroxide concentration (1.5–6 mM H_2O_2/g VSS_o), temperature (55 °C–85 °C) and oxidant dosages (2 additions of 1.5 mM H_2O_2/g VSS_o and 3 additions of 1 mM H_2O_2/g VSS_o).

2.4. Size exclusion chromatographic (SEC) analysis

Biopolymers size distribution (fingerprints) in WAS supernatant was determined through an Agilent 1200 high-performance liquid chromatography (Agilent Technologies Inc., USA), using a Thermo Scientific™ BioBasic™ SEC 300 (4.6 mm × 300 mm) column. The total volume of the column was 4.06 mL (11.59 min), which was estimated by means of a $NaNO_3$ solution. K_2HPO_4 was used as buffer solution at a concentration of 0.1 M, the pH being adjusted to 7. The flowrate was 0.35 mL/min. Prior to injection (20 μl), all the samples were filtered through a Simplepure PVDF/L 0.45 μm filter. A diode array UV detector was employed, using a wavelength of 280 nm.

Calibration column was done with a protein Standard Mix 15–600 kDa (Sigma-Aldrich, 69385), which is composed of four proteins: Ribonuclease A (13.7 kDa), albumin (44.3 kDa), γ-globulin (150 kDa) and thyroglobulin (670 kDa), also including ρ-aminobenzoic acid (0.14 kDa) as low molecular weight marker. The coefficient of determination (R^2) of calibration curve was 0.99. For a better interpretation of obtained results, three molecular size ranges were selected: low (0–15 kDa or 10.36 min–11.59 min), medium (15–150 kDa or 8.22 min–10.36 min) and high (>150 kDa or 0 min–8.22 min). All peaks recorded after the total column elution time were considered as molecules with hydrophobic behaviour. According to other studies, this is usually observed with molecules that interact with the column package due negative charges present in the EPS (Guan et al., 2017; Simon et al., 2009).

2.5. Kinetic models

According to the TH mechanism behind WAS, the increase in temperature improves the decomposition of complex particles into soluble biopolymers, indicating mass transfer due to cell lysis caused by the increase in kinetic energy of the particles (Urrea et al., 2018). Thus, TH kinetics could be described by Eqs. (12) and (13), where *i* is referred to the biopolymers (protein or carbohydrates), $k_{L,VSS}$ and $k_{L,i}$ are the VSS and biopolymer mass transfer coefficient constants (min^{-1}) (Aroniada et al., 2020; Salmi et al., 2013), $C_{VSS\infty}$ and $C_{i\infty}$ are the VSS and biopolymer concentrations (mg/L) after stabilization, while C_{VSS} and C_i are the VSS and biopolymer concentrations (mg/L) at a certain time.

$$-\frac{dC_{VSS}}{dt} = k_{L,VSS}(C_{VSS\infty} - C_{VSS}) \tag{12}$$

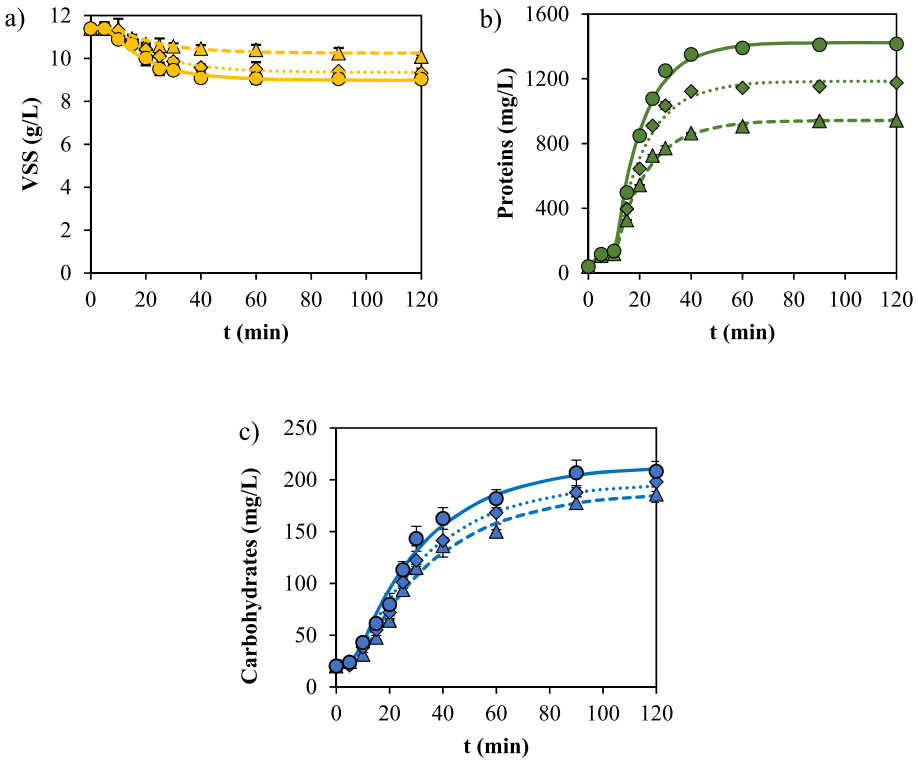

Fig. 1. Evolution of the concentration of VSS (a), proteins (b) and carbohydrates (c) after TH pretreatment at 55 °C (p), 70 °C (u) and 85 °C (l). Experimental data (symbols) and kinetic model (solid, round dotted and square dotted lines) according to equations (12) and (13).

$$\frac{dC_i}{dt} = k_{L,i}(C_{i\infty} - C_i) \quad (13)$$

On the other hand, to analyse the ATH mechanism for each biopolymer, a kinetic model based on the H_2O_2 consumption was proposed.

The suggested kinetic model is based on the hypothesis that VSS were solubilized due to oxidation reactions caused by H_2O_2, releasing biopolymers to the aqueous phase (Bertanza et al., 2015). Hence, the following kinetic equations were proposed:

$$-\frac{dC_{H_2O_2}}{dt} = k_{H_2O_2}\, C_{H_2O_2}^{n_{H_2O_2}} \quad (14)$$

$$-\frac{dC_{VSS}}{dt} = k_{VSS}\, C_{VSS}\, C_{H_2O_2}^{n} \quad (15)$$

$$\frac{dC_i}{dt} = Y_{i/VSS}\, k_{VSS}\, C_{VSS}\, C_{H_2O_2}^{n} \quad (16)$$

The temperature dependence of k_{VSS} can be expressed as follows:

$$k_{VSS} = A_{VSS}\, e^{-Ea_{VSS}/R\,T} \quad (17)$$

H_2O_2 consumption rate is described in Eq. (14), where $k_{H_2O_2}$, $C_{H_2O_2}$ and $n_{H_2O_2}$, are the kinetic constant ($L^{(n_{H_2O_2}-1)}\ mg^{(1-n_{H_2O_2})}\ min^{-1}$), the concentration of H_2O_2 (mg/L) at a certain time and the order of the reaction, respectively. Eq. (15) describes the solubilization of VSS, where k_{VSS} and C_{VSS} are the kinetic constant ($L^n\ mg^{-n}\ min^{-1}$) and the VSS concentration (mg/L) at certain time, respectively, n is the partial order of the reaction with respect to dissolved H_2O_2. Furthermore, an Arrhenius-type temperature dependence for k_{VSS} was assumed, as per Eq. (17), where A_{VSS} ($L^n\ mg^{-n}\ min^{-1}$), Ea_{VSS} (kJ/mol), R (kJ/mol K) and T(K) are the pre-exponential factor, activation energy, the universal gas constant and the process temperature, respectively. For biopolymers (i), Eq. (16) represents their kinetics, where $Y_{i/VSS}$ (mg_i/mg_{VSS}) represents the yield, which is referred to the milligrams of biopolymer released per milligram of VSS solubilized. Micromath Scientist software was employed for the model fitting.

3. Results and discussion

3.1. Thermal hydrolysis (TH) experiments

The results of WAS solubilization in terms of VSS and biomolecule concentrations after being treated by TH at temperatures from 55 to 85 °C are shown in Fig. 1. Besides, the results of TCOD, SCOD, STOC, pH and CN evolution can be found in Fig. S3 in the Supplementary Materials.

A reduction in VSS as well as an increase in SCOD can be seen as temperature rises. It is important to note that the first 10 min are considered a delay, since this is the time needed by the equipment to start the temperature increase. VSS were reduced by 11% after 120 min

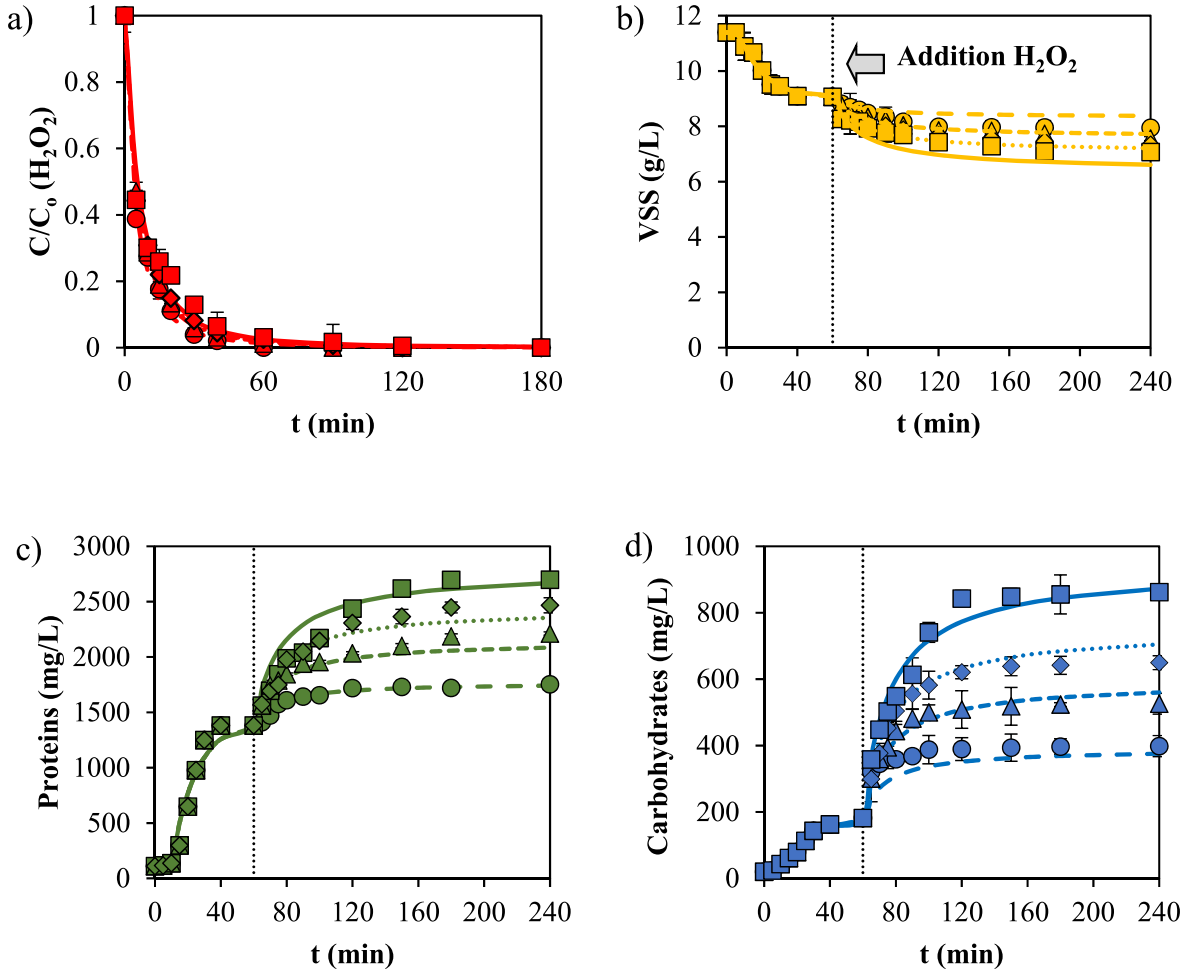

Fig. 2. Evolution of the concentration of H_2O_2 (a), VSS (b), proteins (c) and carbohydrates (d) after ATH pretreatment at 85 °C and H_2O_2 concentrations of: 1.5 mM H_2O_2/gVSS$_o$ (●), 3 mM H_2O_2/gVSS$_o$ (▲),4.5 mM H_2O_2/gVSS$_o$ (◆) and 6 mM H_2O_2/gVSS$_o$ (■). Experimental data (symbols) and kinetic model (solid, round dotted, square dotted and dashed lines) according to equations (14) - (17). Black dotted line marks the transition from TH to ATH (H_2O_2 addition).

of TH at 55 °C, while at 85 °C the reduction was 19% for the same time (Fig. 1a). In the case of SCOD, the concentration increased significantly up to 40 min of treatment, the values being 1.66 ± 0.02 g/L, 2.37 ± 0.03 g/L and 2.73 ± 0.02 g/L for 55 °C, 70 °C and 85 °C, respectively. From that time onwards, SCOD concentration changed slightly, achieving the highest final value (3.00 ± 0.02 g/L) at 85 °C. It should be noted that temperature showed a greater effect than time in terms of floc solubilization. Besides, the low temperatures used did not supply enough kinetic energy to solubilize the cell walls of the WAS (Prorot et al., 2008; Urrea et al., 2017), but mainly affected the extrapolymeric substances (EPS). At this point, it is worthy to mention that solid COD mainly included proteins, carbohydrates and volatile fatty acids. However, the latter are considered the components with the lowest presence (around 10%) (Biswal et al., 2020; Han et al., 2017). Hence, this study was focused on obtaining the main biomolecules with high added value (proteins and carbohydrates).

The evolution of the biopolymers depicted in Fig. 1b–c supported the EPS solubilization mechanism, since protein and carbohydrate concentration at 55 °C for 120 min reached values of 943 ± 8 mg/L (83 mg/gVSS$_o$) and 186 ± 3 mg/L (16 mg/gVSS$_o$), respectively, while at 85 °C for the same time, the value was 46% and 12.5% higher. The amount of biomolecules obtained with TH was similar to that of Biswal et al. (2020), who reported values of 52 mg/gVSS$_o$ and 11 mg/gVSS$_o$ for proteins and carbohydrates, respectively, when saline WAS was treated at 60 °C. The TCOD and the pH trends (Figs. S3a and e) indicate that the hydrolysis of the biopolymers to intermediate compounds was very little, making it necessary to use more severe conditions to achieve their rupture (Khan et al., 1999; Urrea et al., 2017).

As previously mentioned, the temperatures used for TH in this study were high enough for EPS solubilization (Pola et al., 2021). However, they proved to be unsuitable to break the cell walls and take advantage of the intracellular content, which has a greater amount of value-added substances. The concentration of proteins and carbohydrates obtained with TH in this study, were around 80% lower than those achieved with thermal processes using more severe conditions (160 °C and 40 bar) (García et al., 2017; Xue et al., 2015) or oxidizing agents (persulfate or oxygen) (Huang et al., 2020; Lee et al., 2016; Urrea et al., 2017; Wang et al., 2018). Therefore, in order to improve the quantities of biopolymers obtained, H_2O_2 was used as an oxidizing agent, paying special attention to the effect of its concentration, dosing strategy and reaction temperature on biopolymer production.

3.2. Advanced thermal hydrolysis (ATH) experiments

Before conducting ATH tests, an analysis was carried out to determine the H_2O_2 concentration range to be studied. Fig. S1 in the Supplementary Materials revealed that there were no changes in protein concentration above 7.5 mM H_2O_2/g VSS$_o$ at 85 °C, and the same was true for carbohydrates concentration from 6 mM H_2O_2/g VSS$_o$ onwards at the same temperature. Moreover, the effect of H_2O_2 on WAS

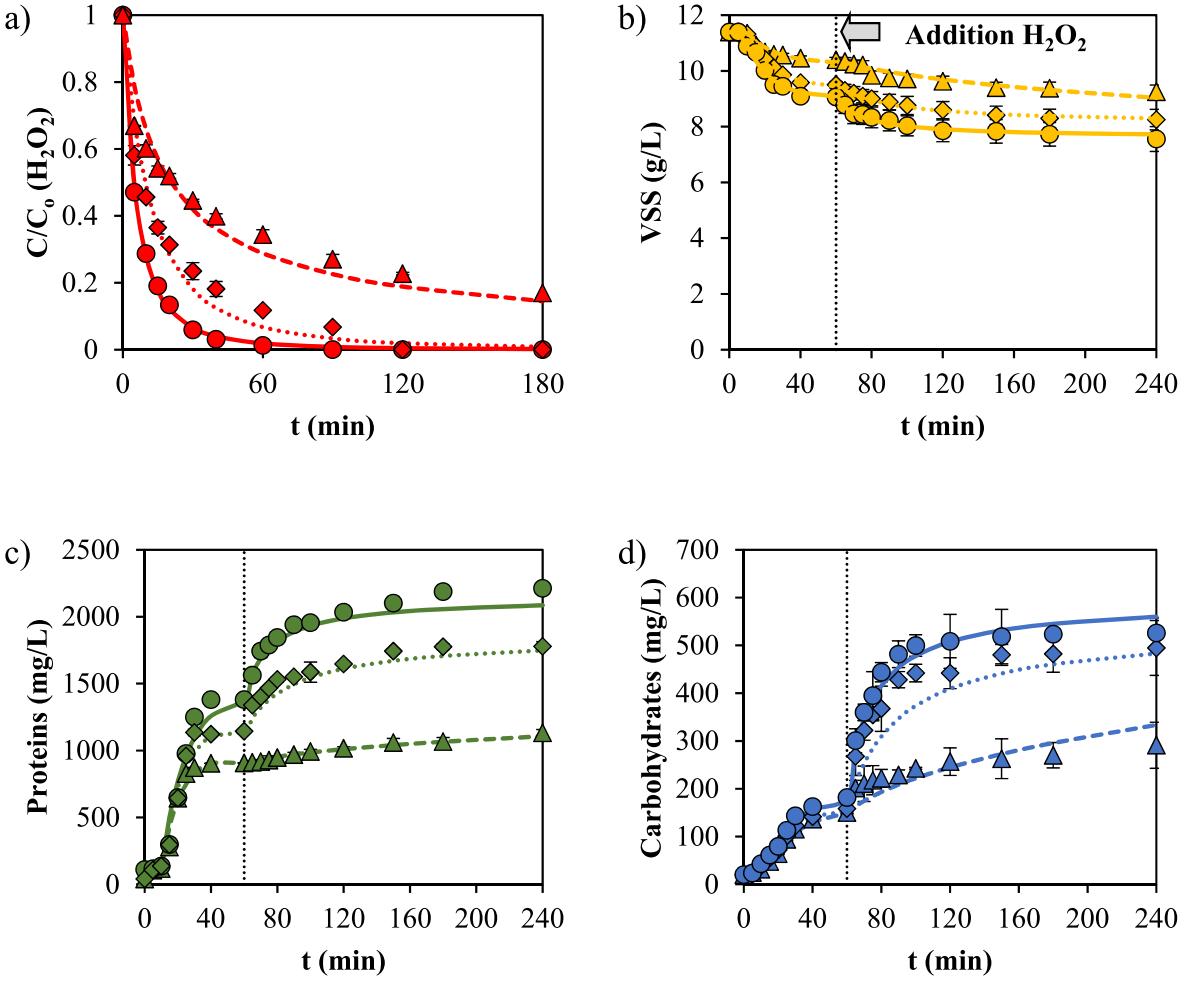

Fig. 3. Evolution of the concentration of H_2O_2 (a), VSS (b), proteins (c) and carbohydrates (d) after ATH pretreatment with 3 mM H_2O_2/gVSS$_o$ at temperatures: 55 °C (▲), 70 °C (◆) and 85 °C (●). Experimental data (symbols) and kinetic model (solid, round dotted and square dotted lines) according to equations (14) - (17). Black dotted line marks the transition from TH to ATH (H_2O_2 addition).

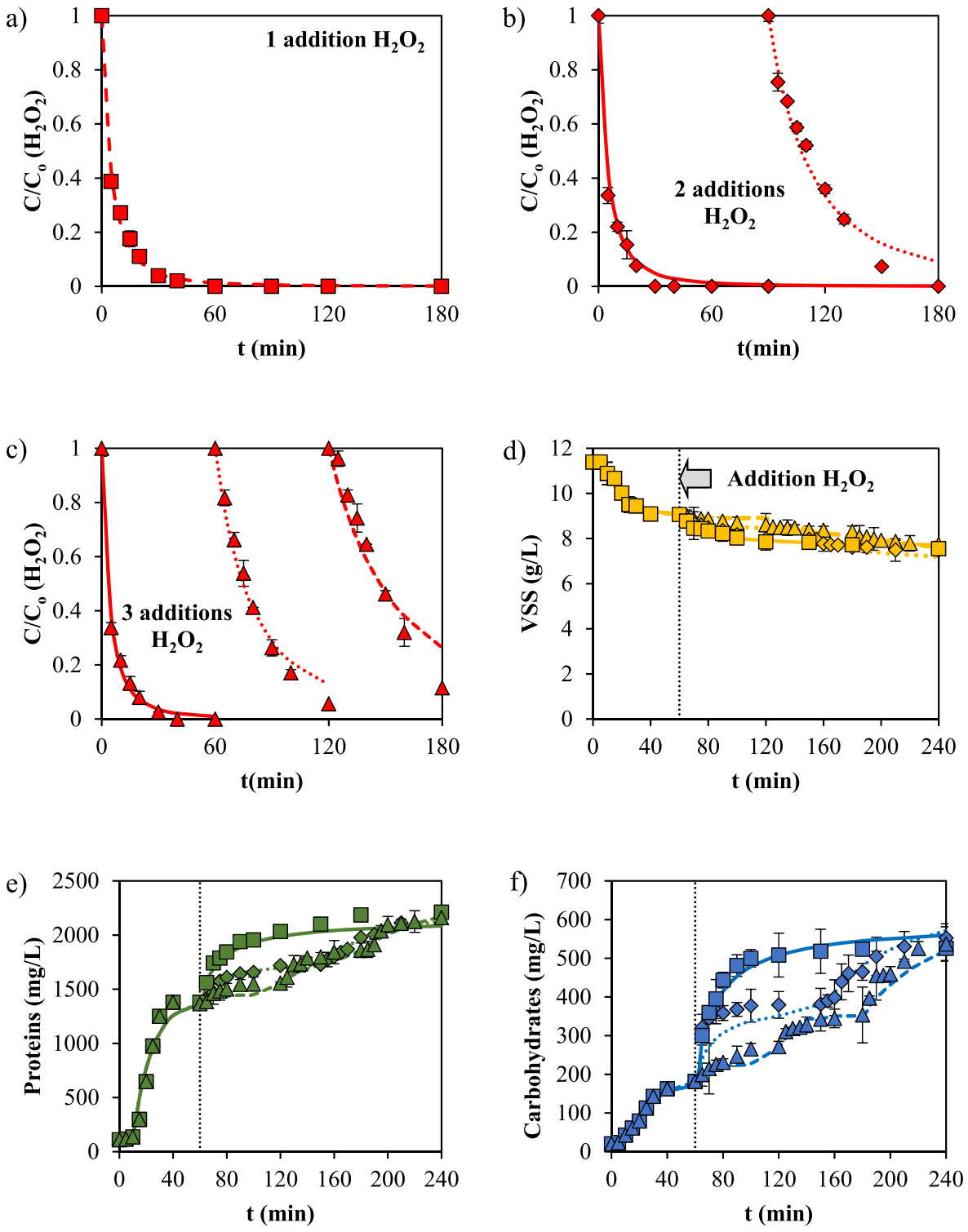

Fig. 4. Evolution of the concentration of H_2O_2 at different additions (a–c), VSS (d), proteins (e) and carbohydrates (f) after ATH pretreatment at 85 °C with 3 additions of 1 mM H_2O_2/g VSS_o (▲), 2 additions of 1.5 mM H_2O_2/g VSS_o (◆) and 1 addition of 3 mM H_2O_2/g VSS_o (■). Experimental data (symbols) and kinetic model (solid, round dotted, and square dotted lines) according to equations (14) - (17). Black dotted line marks the transition from TH to ATH (H_2O_2 addition).

solubilization in absence of temperature was studied in the range 1.5–6 mM H_2O_2/g VSS_o. Thus, the concentration of biomolecules (proteins and carbohydrates) achieved was very low, the maximum values being 202 ± 10 for proteins and 51 ± 1 mg/L for carbohydrates, after 120 min of treatment with 6 mM H_2O_2/g VSS_o (Fig. S2 in the Supplementary Materials). The effect of the temperature on the degradation of H_2O_2 was also analysed. It was found that the concentration of the oxidant remained constant regardless of the temperature value. So, there is no degradation of H_2O_2 due to reaction temperature.

3.2.1. *Effect of H_2O_2 concentration*

The evolution of WAS solubilization due to ATH experiments, adding

Table 2
TH kinetic parameters at temperature range of 55–85 °C, obtained from Eqs. (12) and (13).

	Parameters	Temperature (°C)		
		55	70	85
VSS	$k_{L,VSS}$ (min^{-1})	0.060	0.063	0.068
	$C_{VSS\infty}$ (mg L^{-1})	10249	9353	8985
	R^2	0.9991	0.9997	0.9995
Proteins	$k_{L,i}$ (min^{-1})	0.075	0.079	0.085
	$C_{i\infty}$ (mg L^{-1})	943	1185	11423
	R^2	0.998	0.997	0.998
Carbohydrates	$k_{L,i}$ (min^{-1})	0.033	0.034	0.036
	$C_{i,\infty}$ (mg L^{-1})	189	198	214
	R^2	0.997	0.998	0.997

H_2O_2 in the range of 1.5–6 mM/gVSS_o, is shown in Fig. 2. It is important to note that temperature was 85 °C, and H_2O_2 was added after 60 min of heating, since above that time the concentration of the different parameters and biomolecules achieved a plateau, thus indicating that the TH pretreatment was complete. This allowed us to evaluate the effect of H_2O_2 on ATH properly.

Fig. 2b showed the reduction of VSS. It was found a greater impact on WAS solubilization depending on the addition of H_2O_2. Thus 30% reduction of VSS was obtained when a concentration of 1.5 mM H_2O_2/g VSS_o was used for 120 min, while the reduction was almost 40% after adding 6 mM H_2O_2/g VSS_o for the same reaction time. Besides, SCOD and STOC (Figs. S4b and c in the Supplementary Materials) were also affected as H_2O_2 concentration increased. It should also be noted that the addition of the oxidizing agent contributed to both EPS solubilization and cell wall disruption, thus causing the release of intracellular material into the liquid medium. However, these phenomena (solubilization and disruption) were significant up to 120 min (60 min after H_2O_2 addition), and from that time on, the concentration of the biomolecules and VSS remained practically constant. Fig. 2a showed the evolution of H_2O_2 concentration with time in all of the experiments. As expected, EPS solubilization and cell disruption can be explained based on the reactions shown in Eqs. (1)–(4), which generate oxidative radicals. This led to the complete consumption of H_2O_2 within 60 min when the concentration varied from 1.5 mM H_2O_2/g VSS_o to 6 mM H_2O_2/g VSS_o. Thus, when the H_2O_2 was consumed, there was no further solubilization of WAS.

The evolution of the biomolecules are shown in Fig. 2c–d. It was obtained a significant increase in the concentration of both proteins and carbohydrates due to H_2O_2 addition. Regarding protein concentration, a value of 1754 ± 5 mg/L (154 mg/gVSS_o) was achieved for 60 min when 1.5 mM H_2O_2/gVSS_o was added, while the value was around 1.5 times higher 2697 ± 15 mg/L (237 mg/gVSS_o), when 6 mM H_2O_2/gVSS_o was used at the same reaction time. In the case of carbohydrates, the values reached were lower than those obtained for proteins, ranging from 398 ± 7 ppm (35 mg/gVSS_o) to 862 ± 12 ppm (75 mg/gVSS_o) when H_2O_2 concentrations varied between 1.5 mM H_2O_2/gVSS_o and 6 mM H_2O_2/gVSS_o after 60 min of ATH treatment. However, the effect of H_2O_2 in carbohydrate production was more significant. In this sense, when 6 mM H_2O_2/gVSS_o was added at 85 °C for 60 min, carbohydrate concentration was around 2.2 times higher, while in the case of proteins, it was around 1.5 times higher. These results revealed the existence of a remarkable synergistic effect between thermal hydrolysis and H_2O_2 oxidation when WAS was treated by means of ATH. Thus, the combined effect of these processes in the production of biomolecules was very significant in comparison to that obtained when they were used individually. It should be noted that the production of proteins and carbohydrates was 1376 ± 8 mg/L (121 mg/gVSS_o) and 208 ± 4 mg/L (18 mg/gVSS_o), respectively, when TH was performed at 85 °C 120 min, while the value was 1.9 and 3.1 times higher, respectively, in presence of 4.5 mM H_2O_2/gVSS_o for the same conditions. Therefore, ATH can be considered a suitable option not only for conditioning WAS in terms of manageability (Abelleira

Table 3
Kinetic parameters obtained from Eq. (14)-(17) for the ATH pretreatment of WAS at different temperatures, H_2O_2 concentrations and dosing strategies of H_2O_2.

		Temperature (°C)															
		55		70		85				85							
		H_2O_2 concentration (mM/VSS_o)				H_2O_2 concentration (mM/VSS_o)				H_2O_2 concentration (mM/VSS_o)							
	Parameters	3		3	3	1.5	3	4.5	6	3 1st add.	1.5 1st add.	1.5 2nd add.	1 1st add.	1 2nd add.	1 3rd add.		
H_2O_2	k_{H2O2} ($L^{0.4}$ $mgH_2O_2^{-0.4}$ min^{-1})	0.002		0.004	0.009	0.015	0.009	0.007	0.006	0.009	0.015	0.003	0.020	0.005	0.0025		
	n_{H2O2}								1.4								
	R^2	0.948		0.988	0.9991	0.994	0.9991	0.994	0.980	0.9991	0.994	0.991	0.997	0.995	0.987		
VSS	A_{VSS} ($L^{0.8}$ $mgH_2O_2^{-0.8}$ min^{-1})								3257								
	Ea_{VSS} (kJ/mol)								54								
	k_{vss} ($L^{0.8}$ $mgH_2O_2^{-0.8}$ min^{-1})	$8.53{\cdot}10^{-6}$		$2.02{\cdot}10^{-5}$	$4.46{\cdot}10^{-5}$						$4.46{\cdot}10^{-5}$						
	n								0.8								
	R^2	0.9998		0.9990	0.9990	0.9991	0.9990	0.9990	0.9992	0.9990	0.9992	0.9991	0.9990	0.9990	0.9990		
Proteins	$Y_{i/VSS}$ (mg $mgVSS^{-1}$)	0.214		0.501	0.525						0.525						
	R^2	0.9994		0.996	0.9991	0.998	0.9991	0.998	0.998	0.9991	0.998	0.9990	0.9992	0.9991	0.9995		
Carbohydrates	$Y_{i/VSS}$ (mg $mgVSS^{-1}$)	0.182		0.270	0.282						0.282						
	R^2	0.991		0.999	0.992	0.992	0.992	0.982	0.980	0.992	0.992	0.981	0.997	0.983	0.981		

et al., 2012a, 2012b), but also for the production of high value-added compounds. Furthermore, the mild conditions employed in these experiments could attain energy savings compared to the thermal methods used in other studies. According to the results reported by García et al. (2017), yields of 272 mg/gVSS$_o$ and 106 mg/gVSS$_o$ were achieved for proteins and carbohydrates, respectively. Although such values are slightly higher than the ones obtained in this study, it is important to notice that García et al. (2017) performed thermal hydrolysis under much more severe conditions (160 °C and 40 bar). On the other hand, Lee et al. (2016) used low thermally activated-persulfates (80 °C and 1.8 mM/g VSS$_o$) as oxidants for value-added compound production from WAS and reported values lower than those achieved in this study, these being 27 mg/gVSS$_o$ and 73 mg/gVSS$_o$ for carbohydrates and proteins, respectively, when using peroxymonosulfate; in the case of peroxydisulfate, the attained values were 71 mg/gVSS$_o$ for carbohydrates and 108 mg/gVSS$_o$ for proteins.

Finally, the effect of H_2O_2 addition on the main physicochemical characteristics of WAS, are summarized in Fig. S4 in the Supplementary Materials. While it is true that H_2O_2 is a powerful oxidant, which causes the release of extracellular and intracellular material, the results revealed that higher H_2O_2 concentration also caused a slight decrease in TCOD of WAS, together with a pH decrease. In spite of promoting the partial oxidation of WAS, ATH achieved 20% reduction in TCOD with 6 mM H_2O_2/gVSS$_o$, which is a modest result by comparison with other thermal oxidizing methods; for instance, wet oxidation reached 46% TCOD reduction (Urrea et al., 2018). The reduction of pH from 7.0 to 4.9, was due to the formation of short-chain volatile fatty acids, which are considered as intermediate products in the oxidation of activated sludge (Eskicioglu et al., 2006; Genç et al., 2002).

3.2.2. Temperature effect

The influence of temperature on ATH experiments was analysed in the range 55°C–85 °C. It should be noted that H_2O_2 was added at 60 min after the beginning of the experiment, since after that time on no further changes in biomolecule concentration occurred. H_2O_2, VSS, protein and carbohydrate trends, are depicted in Fig. 3.

The solubilization of the organic matter of WAS due to temperature changes in ATH is shown in Fig. 3a. On viewing the results, ATH had a greater impact on WAS solubilization at higher temperatures. In this sense, the reduction of VSS was 15% at 55 °C for 60 min (after the addition of H_2O_2), while 31% was achieved at 85 °C for the same reaction time. In the case of SCOD (Fig. S5b in the Supplementary Materials), a significant increase with temperature was also observed, the final concentration being 2.91 ± 0.01 mg/L at 55 °C, while the value was 1.6 times higher at 85 °C. Besides, the solubilization effect was also reflected on biomolecule increase (Fig. 3c and d). It should be noted the influence was more noticeable when temperature varied from 55 °C to 70 °C than in the range 70°C-85 °C. In this sense, protein concentration was 1016 ± 11 mg/L (89 mg/gVSS$_o$) at 55 °C for 1 h (after H_2O_2 addition), while at 70 °C and 85 °C at the same time, the values were 1646 ± 6 mg/L (145 mg/gVSS$_o$) and 2034 ± 14 mg/L (179 mg/gVSS$_o$). This implied 62% increase in the 55°C-70 °C range and only 23.5% from 70 °C to 85 °C. This was also observed in the case of carbohydrates, in which 72% increase was observed between 55°C-70 °C and only 15% in the range 70 °C to 85 °C (carbohydrate concentration: 257 ± 9 mg/L (23 mg/gVSS$_o$) at 55 °C for 1 h after H_2O_2 addition). This can be explained due to the effect of EPS, which act as a three-dimensional gel-like hydrated matrix (Simon et al., 2009), hampering the release of intracellular material to the liquid phase due to the low thermal energy used. It is interesting to point out that the reactivity of H_2O_2 is fostered by temperature rise, as hydroperoxyl, alkyl and hydroxyl radicals are generated at a faster rate. Thus, the consumption of H_2O_2 over time (Fig. 3a), was quicker as temperature increased, thus being complete at 90 min and 120 min, for 85 °C and 70 °C, respectively. However, at 55 °C, H_2O_2 was still present in the reaction media (WAS liquid phase) by the end of the experiment. Previous studies suggested that the thermal energy supplied to ATH processes significantly increased the reactivity of H_2O_2 and water, which firstly acted on the EPS and, on a subsequent stage on the cell walls, which contains a higher percentage of biopolymers, especially proteins (Brunner, 2009; Ngo et al., 2021; Toor et al., 2011; Urrea et al., 2017). In this study, the yields of the biopolymers were higher than those reported by Lee et al. (2016), who obtained values from 28 to 78 mg/gVSS$_o$ for proteins and 42–56 mg/gVSS$_o$ for carbohydrates when 1.8 mM/gVSS$_o$ of persulfates (peroxymonosulfate and peroxydisulfate) were used as oxidants activated at 50 °C and 80 °C.

Regarding the possible WAS partial oxidation due to H_2O_2 addition, no significant changes were observed with temperature variation. In this sense, the value of TCOD concentration decreased 9% and 12% for 180 min (after H_2O_2 addition), when temperature was 55 °C and 85 °C, respectively, the initial value being 17.48 ± 0.01 g/L. Therefore, it can be concluded that the fraction of WAS solubilized and fully mineralized can be considered small at the lower temperatures employed (Abelleira et al., 2012b).

3.2.3. Dosing strategy effect

The impact of ATH on WAS pretreatment with different H_2O_2 dosing schemes was also examined (Fig. 4 and Fig. S6 in the Supplementary Materials). It should be noted that H_2O_2 was added at 60 min after the beginning of the experiment when 1 addition of 3 mM H_2O_2/g VSS$_o$ was performed, while it was added at 60 min and 90 min, and at 60 min, 120 min and 180 min, when 2 additions of 1.5 mM H_2O_2/g VSS$_o$ and 3 additions of 1 mM H_2O_2/g VSS$_o$, respectively, were carried out. In terms of solubilization, no major differences were observed in VSS reduction and SCOD increase at the end of the experiment. However, when H_2O_2 was added once, both VSS and SCOD concentrations reached a constant value in 120 min, while in the case of 3 additions, it was achieved in 185 min. Besides, H_2O_2 was completely consumed within 60 min in all the first additions regardless of the initial concentration, while in the second and third additions the consumption rate was lower. This suggests that during WAS solubilization, two fractions can be considered, one of them being easily oxidizable and other more refractory to oxidation. In this sense, when H_2O_2 was added in just one addition, both fractions could be solubilized (firstly the easily oxidizable and then, the more difficult one), since the oxidant was in excess. Nevertheless, when lower concentrations of H_2O_2 were added, it is considered that in the first addition only the easily oxidizable fraction was solubilized quickly but no the refractory one, since all oxidant was consumed, thus explaining why H_2O_2 decomposition was fast. When subsequent H_2O_2 additions were conducted, only the hardly oxidizable fraction remained to be solubilized, which resulted in lower kinetic constants. Thus, the value of k_{H2O2} for the first addition of 1 mM H_2O_2/g VSS$_o$ was 0.020 $L^{0.4}$ $mgH_2O_2^{-0.4}$ min^{-1}, while it was 4.3 and 8 times lower for the second and third additions, respectively. This was also observed when 1.5 mM H_2O_2/g VSS$_o$ was added, the value of the k_{H2O2} being 0.015 $L^{0.4}$ $mgH_2O_2^{-0.4}$ min^{-1} for the first addition and 0.003 $L^{0.4}$ $mgH_2O_2^{-0.4}$ min^{-1} for the second one (see Table 3 in section 3.4 related to kinetic model).

Regarding the evolution of proteins and carbohydrates, the final concentration was practically the same regardless of the dosing strategy, the values being 2162 ± 8 mg/L (90 mg/gVSS$_o$) and 553 ± 44 mg/L (49 mg/gVSS$_o$), respectively. However, it can also be observed that their concentration increased rapidly and reached a plateau in 60 min after one addition of H_2O_2, while their concentration rose more slowly after 2 or 3 additions, reaching a plateau in less than half of time. On viewing TCOD values (Fig. S6a), it can also be stated that there was a partial WAS oxidation due to the non-selective action of H_2O_2. This can be explained considering the formation of carboxylic acids, since pH values decreased throughout the pretreatment and STOC reached a plateau and remained constant. The production of carboxylic acids from oxidised WAS was also reported by other authors (Kim et al., 2016).

3.3. Size distribution of biopolymers after TH and ATH experiments

In the previous sections, the evolution of biomolecules after WAS pretreatment using TH and ATH was discussed in detail. However, the influence on their size distribution is also important, since it can be highly useful depending on biopolymer application. For this reason, the fingerprints of the solubilized biopolymers were determined.

Fig. S7 (Supplementary Materials) shows the evolution of the fingerprints for TH experiments at temperatures between 55 °C and 85 °C. They were classified in four categories to explain it more thoroughly: i) high (>150 kDa), ii) medium (15–150 kDa), iii) low (<15 kDa), those three included in the size exclusion zone and iv) area out of the total volume of the column, which corresponded to hydrophobic compounds that interact with column filling material (Urrea et al., 2018). On viewing the results, the use of low temperatures allowed obtaining high and medium-sized molecules. Besides, the rise in temperature caused a rapid shortening of the higher biopolymers (>150 kDa). In this sense, the area was around 0.2 AU*s for 10 min at 55 °C, while it was 2.5 times lower at 70 °C for the same time. On the other hand, the reduction of high and medium-sized molecules allowed the appearance of low-sized ones and mainly compounds that interact with the column; the latter are generally associated with the presence of proteins, which can exhibit a great hydrophobic behaviour (Liu and Fang, 2003). Thus, the area of the hydrophobic molecules was around 5.2 AU*s for 30 min at 55 °C, while it was 65% higher at 85 °C for the same time. Besides, it was also reported that non-oxidative heat treatments cause protein fibrillation, thereby reducing its hydrophilicity (Seviour et al., 2019), which is in agreement with the increase in the hydrophobic compounds observed.

With regards to fingerprints evolution in ATH, the effect of H_2O_2 concentration on WAS will be discussed first. Fig. S8 (Supplementary Materials) depicts particle size distribution after adding H_2O_2 concentrations in the 1.5–6 mM H_2O_2/g VSS_o range. It should be noted that the remarkable change obtained in all particle sizes just after the addition of the oxidant. Thus, the hydrophobic compounds decreased significantly as H_2O_2 concentration increases, reaching reductions of 22%, when 1.5 mM H_2O_2/g VSS_o were added, while it was 66% with 6 mM H_2O_2/g VSS_o, respectively. Urrea et al. (2018) also reported a lower presence of hydrophobic compounds when using wet oxidation in comparison to thermal hydrolysis treatment at 160 °C and 40 bar. This can be due to the oxidation reactions, which promote the transformation of hydrophobic compounds such as proteins or lipids, into hydrophilic compounds, which presented low and medium sizes. This was more marked when lower concentrations of H_2O_2 was used, which can be explained considering that the oxidant mainly oxidised the biopolymers present in the reaction medium. However, when higher concentrations of H_2O_2 were added, two effects can be considered, the breakdown of EPS and cell walls which causes the increases of low-sized molecules and hydrophobic compounds and the partial modification/oxidation of some of the functional groups of the biopolymers, thus altering their hydrophobic nature (Urrea et al., 2016b).

The analysis of the fingerprints at temperatures between 55 °C and 85 °C when 3 mM H_2O_2/g VSS_o was added (Fig. S9 in Supplementary Materials), revealed that it was necessary higher temperatures (70 °C and 85 °C) to observe the decrease in the amount of hydrophobic molecules after addition of the oxidant. Thus, the area of hydrophobic compounds was around 7.7 AU*s, for 5 min after the addition of H_2O_2 at 55 °C, respectively, while, the values were 1.4 times and 2.3 times lower, respectively, when temperature was 70 °C and 85 °C. This suggested that a minimum temperature was required in order for the modification of the hydrophobic compounds to take place. In this case, their modification also implied the rise in low-sized and medium-sized molecules, the values being at 85 °C, 1.8 times and 5 times higher, respectively, than those obtained at 55 °C.

Finally, the measurement of the fingerprints was carried out after adding different dosages of H_2O_2 (3 additions of 1 mM H_2O_2/g VSS_o, 2 additions of 1.5 mM H_2O_2/g VSS_o and 1 additions of 3 mM H_2O_2/g VSS_o) throughout the experiment. On viewing Fig. S10 (Supplementary Materials), it can be indicated that each of the H_2O_2 addition led to the drop in the hydrophobic compounds and the corresponding rise in low-sized and medium-sized compounds, regardless of the amount of oxidant used. It should be noted that this rise was more significant when 1 mM H_2O_2/g VSS_o was added and, in particular, during the first addition. Thus, the areas for the low-sized and medium-sized compounds after 5 min of the first addition of H_2O_2, were around 1.6 and 2.4 times higher than those attained when 3 mM H_2O_2/g VSS_o was added at the same time (low-sized and medium-sized compound areas: 1.1 AU*s and 4.5 AU*s). As it was previously indicated, this suggested a partial modification/oxidation of some of the functional groups of the biopolymers present in the reaction media at low oxidant concentration and the existence of two effects at higher concentrations, thus implying simultaneous solubilization of EPS and cell walls and the modification of the functional groups of the hydrophobic biopolymers solubilized changing their nature to more hydrophilic one (Urrea et al., 2016b).

3.4. Kinetic model

Table 2 shows the kinetic parameters for TH in a temperature range from 55 °C to 85 °C. Solid, dotted and dashed lines in Fig. 1 denoted model curves according to Eqs. (12) and (13). As expected, a rise in the temperature accelerated the solubilization kinetics of VSS and biopolymers. In this sense, the mass transfer coefficients for VSS, proteins and carbohydrates were 0.060, 0.075 and 0.033 min^{-1}, respectively, at 55 °C, the values being around 14%, 13% and 10% higher than those obtained at 85 °C. Besides, the solubilization of proteins was faster than for carbohydrates, their kinetic constants being around 2.3 times higher than those obtained for carbohydrates, which varied from 0.033 to 0.036 min^{-1} between 55 °C and 85 °C.

Table 3 sums up the kinetic parameters obtained for the ATH pretreatment of WAS. Solid, dotted and dashed lines in Figs. 2–4 denoted model curves according to Eq. (14)-(17). It should be noted that the values of k_{VSS} significantly increased with temperature, this being 5.2 times higher at 85 °C than that obtained at 55 °C ($8.53{\cdot}10^{-6}$ $L^{0.4}$ $mgH_2O_2^{-0.4}$ min^{-1}). Regarding the values of $Y_{i/VSS,}$ they were coherent with the concentration of biopolymers solubilized, thus obtaining higher values of this fitting parameter when higher concentrations of biopolymers were obtained. Moreover, the yields at 70 °C (0.501 mg/mg VSS) and 85 °C (0.525 mg/mg VSS) indicated that proteins were the main product obtained after ATH pretreatment. These results were in agreement with those reported by Urrea et al. (2017), in which higher values of $Y_{i/VSS}$ were reported for proteins (0.492 mg/mg VSS) than for carbohydrates (0.2 mg/mg VSS) when sludge was oxidised by wet oxidation. Besides, the yield per milligram of VSS also increased with the rise in the temperature. This effect being more marked in the 55°C-70 °C range than in the 70°C-85 °C one for both biopolymers. In the case of proteins, $Y_{i/VSS}$ was around 2.3 and 2.5 times higher at 70 °C and 85 °C, respectively, than that obtained at 55 °C (0.214 mg/mg VSS). Considering the value of the activation energy, it is very similar to that reported by Urrea et al. (2014), who obtained 53 kJ/mol for the solubilization phase of the sludge using wet oxidation. This value lied far below the one needed for the mineralization of the already dissolved compounds (178 kJ/mol) (Shende and Levec, 1999).

4. Conclusions

The use of ATH for the production of high value-added biomolecules (proteins and carbohydrates) from WAS can be considered an interesting technology. The results obtained revealed the existence of a synergistic effect between TH and H_2O_2 oxidation, when WAS was treated by means of ATH. Thus, the production of proteins and carbohydrates was 2407 ± 58 mg/L (211 mg/gVSS_o) and 621 ± 19 mg/L (54 mg/gVSS_o), respectively, when ATH was performed at 85 °C with 4.5 mM H_2O_2/gVSS_o for 120 min, while the value was 1.9 and 3.1 times lower, respectively, in

absence of the oxidant. Besides, ATH had a greater impact on WAS solubilization when high temperatures and H_2O_2 concentrations were used. The addition of H_2O_2 had a significant effect on the size distribution of the biomolecules, and led to the transformation of hydrophobic compounds, such as proteins or lipids, into low-sized and medium-sized hydrophilic compounds. The analysis of the kinetics of VSS solubilization revealed that the values of k_{VSS} significantly increased with temperature, this being 5.2 times higher at 85 °C than that obtained at 55 °C ($8.53 \cdot 10^{-6}$ $L^{0.8}$ $mgH_2O_2^{-0.8}$ min^{-1}). Moreover, the values of k_{H2O2} obtained when different dosing strategies were employed suggested the presence of two fractions during WAS solubilization, one of them being easily oxidizable and other more refractory to oxidation.

Declaration of competing interest

The authors declare that they have no known competing financial interests or personal relationships that could have appeared to influence the work reported in this paper.

Data availability

Data will be made available on request.

Acknowledgements

The authors would like to thank the financial support from the Science, Innovation and University Office of Principality of Asturias (Spain) through the project GRUPIN AYUD/2021/51041. Authors also acknowledge the financial support from the State Research Agency (Spanish Ministry of Science, Innovation and Universities) through the projects MCIU-19-RTI2018-094218-B-I00 and MCIU-22-PID2021-125942OB-I00. L. Romero acknowledges the FPI grant (PRE2019-091054).

Appendix A. Supplementary data

Supplementary data to this article can be found online at https://doi.org/10.1016/j.jenvman.2023.118243.

References

Abe, N., Tang, Y.-Q., Iwamura, M., Morimura, S., Kida, K., 2013. Pretreatment followed by anaerobic digestion of secondary sludge for reduction of sewage sludge volume. Water Sci. Technol. 67, 2527–2533.
Abelleira, Pérez-Elvira, S.I., Portela, J.R., Sánchez-Oneto, J., Nebot, E., 2012a. Advanced thermal hydrolysis: optimization of a novel thermochemical process to aid sewage sludge treatment. Environ. Sci. Technol. 46, 6158–6166.
Abelleira, Pérez-Elvira, S.I., Sánchez-Oneto, J., Portela, J.R., Nebot, E., 2012b. Advanced Thermal Hydrolysis of secondary sewage sludge: a novel process combining thermal hydrolysis and hydrogen peroxide addition. Resour. Conserv. Recycl. 59, 52–57.
APHA, 2012. Standard Methods for Examination of Water and Wastewater. American Public Health Association, Washington.
Appels, L., Baeyens, J., Degrève, J., Dewil, R., 2008. Principles and potential of the anaerobic digestion of waste-activated sludge. Prog. Energy Combust. Sci. 34, 755–781.
Aroniada, M., Maina, S., Koutinas, A., Kookos, I.K., 2020. Estimation of volumetric mass transfer coefficient (kLa)—review of classical approaches and contribution of a novel methodology. Biochem. Eng. J. 155, 107458.
Bachir, S., Barbati, S., Ambrosio, M., Tordo, P., 2001. Kinetics and mechanism of wet-air oxidation of nuclear-fuel-chelating compounds. Ind. Eng. Chem. Res. 40, 1798–1804.
Bertanza, G., Galessi, R., Menoni, L., Salvetti, R., Slavik, E., Zanaboni, S., 2015. Wet oxidation of sewage sludge: full-scale experience and process modeling. Environ. Sci. Pollut. Control Ser. 22, 7306–7316.
Biswal, B., Huang, H., Dai, J., Chen, G.-H., Wu, D., 2020. Impact of low-thermal pretreatment on physicochemical properties of saline waste activated sludge, hydrolysis of organics and methane yield in anaerobic digestion. Bioresour. Technol. 297, 122423.
Brunner, G., 2009. Near critical and supercritical water. Part I. Hydrolytic and hydrothermal processes. J. Supercrit. Fluids 47, 373–381.
Chen, Y., Jiang, S., Yuan, H., Zhou, Q., Gu, G., 2007. Hydrolysis and acidification of waste activated sludge at different pHs. Water Res. 41, 683–689.
DuBois, Michel, Gilles, K.A., Hamilton, J.K., Rebers, P.A., Smith, Fred, 1956. Colorimetric method for determination of sugars and related substances. Anal. Chem. 28, 350–356.
Elshikh, M.S., Hussein, D.S., Al-khattaf, F.S., Rasheed El-Naggar, R.A., Almaary, K.S., 2022. Diclofenac removal from the wastewater using activated sludge and analysis of multidrug resistant bacteria from the sludge. Environ. Res. 208, 112723.
Erden, G., Filibeli, A., 2010. Improving anaerobic biodegradability of biological sludges by Fenton pre-treatment: effects on single stage and two-stage anaerobic digestion. Desalination 251, 58–63.
Eskicioglu, C., Kennedy, K.J., Droste, R.L., 2006. Characterization of soluble organic matter of waste activated sludge before and after thermal pretreatment. Water Res. 40, 3725–3736.
Gao, J., Weng, W., Yan, Y., Wang, Y., Wang, Q., 2020. Comparison of protein extraction methods from excess activated sludge. Chemosphere 249, 126107.
García, M., Urrea, J.L., Collado, S., Oulego, P., Díaz, M., 2017. Protein recovery from solubilized sludge by hydrothermal treatments. Waste Manag. 67, 278–287.
Genç, N., Yonsel, Ş., Dağaşan, L., Onar, A.N., 2002. Wet oxidation: a pre-treatment procedure for sludge. Waste Manag. 22, 611–616.
Geng, H., Xu, Y., Zheng, L., Liu, H., Dai, X., 2022. Cation exchange resin pretreatment enhancing methane production from anaerobic digestion of waste activated sludge. Water Res. 212, 118130.
Guan, R., Yuan, X., Wu, Z., Wang, H., Jiang, L., Li, Y., Zeng, G., 2017. Functionality of surfactants in waste-activated sludge treatment: a review. Sci. Total Environ. 609, 1433–1442.
Han, Y., Zhuo, Y., Peng, D., Yao, Q., Li, H., Qu, Q., 2017. Influence of thermal hydrolysis pretreatment on organic transformation characteristics of high solid anaerobic digestion. Bioresour. Technol. 244, 836–843.
Huang, H., Guo, G., Tang, S., Li, B., Li, J., Zhao, N., 2020. Persulfate oxidation for alternative sludge treatment and nutrient recovery: an assessment of technical and economic feasibility. J. Environ. Manag. 272, 111007.
Hwang, J., Zhang, L., Seo, S., Lee, Y.-W., Jahng, D., 2008. Protein recovery from excess sludge for its use as animal feed. Bioresour. Technol. 99, 8949–8954.
Jeong, S.Y., Chang, S.W., Ngo, H.H., Guo, W., Nghiem, L.D., Banu, J.R., Jeon, B.-H., Nguyen, D.D., 2019. Influence of thermal hydrolysis pretreatment on physicochemical properties and anaerobic biodegradability of waste activated sludge with different solids content. Waste Manag. 85, 214–221.
Kacprzak, M., Neczaj, E., Fijałkowski, K., Grobelak, A., Grosser, A., Worwag, M., Rorat, A., Brattebo, H., Almås, Å., Singh, B.R., 2017. Sewage sludge disposal strategies for sustainable development. Environ. Res. 156, 39–46.
Khan, Y., Anderson, G.K., Elliott, D.J., 1999. Wet oxidation of activated sludge. Water Res. 33, 1681–1687.
Kim, M.S., Lee, K.M., Kim, H.E., Lee, H.J., Lee, Changsoo, Lee, Changha, 2016. Disintegration of waste activated sludge by thermally-activated persulfates for enhanced dewaterability. Environ. Sci. Technol. 50, 7106–7115.
Lee, K.M., Kim, M.S., Lee, C., 2016. Oxidative treatment of waste activated sludge by different activated persulfate systems for enhancing sludge dewaterability. Sustainable Environment Research 26, 177–183.
Liu, Y., Fang, H.H.P., 2003. Influences of extracellular polymeric substances (EPS) on flocculation, settling, and dewatering of activated sludge. Crit. Rev. Environ. Sci. Technol. 33, 237–273.
Lowry, OliverH., Rosebrough, NiraJ., Farr, A.L., Randall, RoseJ., 1951. Protein measurement with the folin phenol reagent. J. Biol. Chem. 193, 265–275.
Ngo, P.L., Udugama, I.A., Gernaey, K.V., Young, B.R., Baroutian, S., 2021. Mechanisms, status, and challenges of thermal hydrolysis and advanced thermal hydrolysis processes in sewage sludge treatment. Chemosphere 281, 130890.
Nogueira, R., Oliveira, M., Paterlini, W., 2005. Simple and fast spectrophotometric determination of H2O2 in photo-Fenton reactions using metavanadate. Talanta 66, 86–91.
Pathak, A., Dastidar, M.G., Sreekrishnan, T.R., 2009. Bioleaching of heavy metals from sewage sludge: a review. J. Environ. Manag. 90, 2343–2353.
Pilli, S., Yan, S., Tyagi, R.D., Surampalli, R.Y., 2015. Thermal pretreatment of sewage sludge to enhance anaerobic digestion: a review. Crit. Rev. Environ. Sci. Technol. 45, 669–702.
Pola, L., Fernández-García, L., Collado, S., Oulego, P., Díaz, M., 2021. Macronutrient solubilisation during hydrothermal treatment of sewage sludge. J. Water Process Eng. 43, 102270.
Prorot, A., Eskicioglu, C., Droste, R., Dagot, C., Leprat, P., 2008. Assessment of physiological state of microorganisms in activated sludge with flow cytometry: application for monitoring sludge production minimization. J. Ind. Microbiol. Biotechnol. 35, 1261–1268.
Qiao, S., Hou, C., Wang, X., Zhou, J., 2020. Minimizing greenhouse gas emission from wastewater treatment process by integrating activated sludge and microalgae processes. Sci. Total Environ. 732, 139032.
Rivas, F.J., Kolaczkowski, S.T., Beltran, F.J., McLurgh, D.B., 1999. Hydrogen peroxide promoted wet air oxidation of phenol: influence of operating conditions and homogeneous metal catalysts. J. Chem. Technol. Biotechnol. 74, 390–398.
Salmi, T., Grénman, H., Wärnå, J., Murzin, D.Yu, 2013. New modelling approach to liquid–solid reaction kinetics: from ideal particles to real particles. Chem. Eng. Res. Des. 91, 1876–1889.
Seviour, T., Derlon, N., Dueholm, M.S., Flemming, H.-C., Girbal-Neuhauser, E., Horn, H., Kjelleberg, S., van Loosdrecht, M.C.M., Lotti, T., Malpei, M.F., Nerenberg, R., Neu, T. R., Paul, E., Yu, H., Lin, Y., 2019. Extracellular polymeric substances of biofilms: suffering from an identity crisis. Water Res. 151, 1–7.
Shende, R.V., Levec, J., 1999. Wet oxidation kinetics of refractory low molecular mass carboxylic acids. Ind. Eng. Chem. Res. 38, 3830–3837.

Shi, X., Zhu, L., Li, B., Liang, J., Li, X., 2021. Surfactant-assisted thermal hydrolysis off waste activated sludge for improved dewaterability, organic release, and volatile fatty acid production. Waste Manag. 124, 339–347.
Simon, S., Païro, B., Villain, M., D'Abzac, P., Hullebusch, E., Van Lens, P., Guibaud, G., 2009. Evaluation of size exclusion chromatography (SEC) for the characterization of extracellular polymeric substances (EPS) in anaerobic granular sludges. Bioresour. Technol. 100, 6258–6268.
Tekin, K., Karagöz, S., Bektaş, S., 2014. A review of hydrothermal biomass processing. Renew. Sustain. Energy Rev. 40, 673–687.
Toor, S.S., Rosendahl, L., Rudolf, A., 2011. Hydrothermal liquefaction of biomass: a review of subcritical water technologies. Energy 36, 2328–2342.
Urrea, J.L., Collado, S., Laca, A., Díaz, M., 2014. Wet oxidation of activated sludge: transformations and mechanisms. J. Environ. Manag. 146, 251–259.
Urrea, J.L., Collado, S., Oulego, P., Díaz, M., 2016a. Effect of wet oxidation on the fingerprints of polymeric substances from an activated sludge. Water Res. 105, 282–290.
Urrea, J.L., Collado, S., Oulego, P., Díaz, M., 2016b. Effect of wet oxidation on the fingerprints of polymeric substances from an activated sludge. Water Res. 105, 282–290.
Urrea, J.L., Collado, S., Oulego, P., Díaz, M., 2017. Formation and degradation of soluble biopolymers during wet oxidation of sludge. ACS Sustain. Chem. Eng. 5, 3011–3018.
Urrea, J.L., García, M., Collado, S., Oulego, P., Díaz, M., 2018. Sludge hydrothermal treatments. Oxidising atmosphere effects on biopolymers and physical properties. J. Environ. Manag. 206, 284–290.
Wang, H., Cai, W.W., Liu, W.Z., Li, J.Q., Wang, B., Yang, S.C., Wang, A.J., 2018. Application of sulfate radicals from ultrasonic activation: disintegration of extracellular polymeric substances for enhanced anaerobic fermentation of sulfate-containing waste-activated sludge. Chem. Eng. J. 352, 380–388.
Xue, Y., Liu, H., Chen, S., Dichtl, N., Dai, X., Li, N., 2015. Effects of thermal hydrolysis on organic matter solubilization and anaerobic digestion of high solid sludge. Chem. Eng. J. 264, 174–180.